GEOMETRY EFFECTS ON THERMOHYDRAULIC BEHAVIOR OF FLUID FLOW IN A SQUARE ENCLOSURE WITH AN INNER CIRCULAR TUBE

A. Ahmadi Nadooshan[1*], A. Jahanbakhshi[1], M. Bayareh[1]

ABSTRACT

Convective heat transfer in non-circular channels are of interest in many industrial applications. In the present work, fluid flow in the space between a square channel and a circular tube with different positions of the holder rigid plate is investigated numerically. The use of holder plates is applicable in industrial applications. Holder plates allow different flows with different thermal and hydrodynamic behaviors in a channel at constant Reynolds numbers. Six geometries selected to explore the effect of the position of holder plate on heat transfer rate. Results demonstrated that the plate position has significant effects on fluid flow behavior. It is found that hydrodynamic and thermal behavior affected by the plate position for different Reynolds numbers. For example, for the case that the circular tube is positioned in the center of the square channel with two inclined plates, average convective heat transfer outside and between the two plates is 344 $[\frac{w}{m^2k}]$ and 465 $[\frac{w}{m^2k}]$, respectively.

Keywords: *Square Channel, Forced Convection, Numerical Simulation, Holder Rigid Plate, Reynolds Number*

INTRODUCTION

Regarding great application of non-circular sections in many engineering areas, some researchers investigated heat transfer in laminar fluid flows in such cross-sections. Due to limited contact surface area between the fluid and the wall, heat transfer is low in these channels. As a result, the rate of shear stress from contact between the fluid and channel wall is lower in the flowing fluid. Therefore, pressure drop in these channels is lower than that in circular ones. Low pressure drop in these sections emphasizes their importance in industrial applications. Moreover, reduced contact surface area between the fluid and walls reduces convective heat transfer. Today, increasing heat transfer is investigated to design smaller heat exchangers. Since non-circular sections, such as square and triangular channels, are associated with pressure drop reduction in passing fluids, they should be considered for investigation. Choi [1] was the first one who used fluids containing a suspension of nanoparticles and investigated their significant thermal properties through measuring convective heat transfer. Murshed and Castro [2] investigated forced convection for various nanofluids and addressed different base fluids, such as water, ethylene glycol, and engine oil, and found out that nanofluids have higher heat transfer coefficient in comparison with the base fluids.

Mirmasoumi and Behzadmehr [3] investigated laminar mixed convection of water-aluminum oxide in a horizontal circular tube using a two-phase mixture model. Results indicated that although nanoparticles have no effect on hydrodynamic parameters of flow in the fully developed region, they significantly affect thermal parameters. Pishkar and Ghasemi [4] investigated mixed convection of nano and pure fluids in a horizontal channel containing a heat source using a single-phase numerical method. They showed that the application of nanofluid improves the distribution of heat and increases mean temperature of the heat source. Vasefi and Alizadeh [5] investigated the effect of CuO-water nanofluid on forced convection of water flow in horizontal channels with different cross-sections using the two-phase Euler-Lagrange method. Their results indicated that heat transfer increases due to the use of nanoparticles.

Zeinali et al. [6] investigated heat transfer from nanofluids in channels with triangular and equilateral sections and found that lower pressure drop occurs in triangular cross-section in comparison with other cross-sections. In addition, their results showed that heat transfer intensity depends on the volume fraction of nanoparticles. Effects of estimation error in effective dynamic viscosity and conductivity of aluminum-water nanofluid on free convective heat transfer in a heated square enclosure was studied by Ho et al. [7]. They showed that the heat transfer intensity in the middle of the enclosure (cavity) could be determined using dynamic

viscosity equation by referring to the base fluid. Mansour et al. [8] simultaneously investigated the laminar-mixed convection and heat transfer of aluminum oxide-water nanofluid in a tube with its wall exposed to uniform heat flux. Nguyen et al. [9] performed a study on convective heat transfer of aluminum oxide-water nanofluid in the process of cooling electronic components. They showed that a nanofluid with 36 nm particle size provides higher convective heat transfer than the one with 47 nm particle size. Heris et al. [10] numerically investigated laminar convective heat transfer of a nanofluid in a tube under a constant temperature boundary condition. Shah and London [11] studied heat transfer properties of a laminar flow in channels with different shapes, including a channel with an equilateral triangle cross-section, a channel with an equilateral triangle cross-section and rounded edges, and channels with equilateral triangle and right triangle cross-sections in a various range of heat boundary conditions. Zhang [12] studied convective heat transfer from laminar fully-developed flows at different Reynolds numbers from hydrodynamic and thermal perspectives in ducts with triangle and equilateral triangle cross-sections, uniform wall temperature, and apex angles from 30° to 120°. Results demonstrated that the Nusselt number of nanofluid increases by increasing the concentration of nanoparticles and reducing their diameter. Heyhat and Kowsary [13] investigated the effect of non-uniform distribution of nanoparticles on flow and thermal parameters of water-alumina nanofluid in a circular tube. They indicated that non-uniform distribution of nanoparticles improves the heat transfer. Kalteh and Mehrzad [14] numerically investigated laminar flow heat transfer of a nanofluid in a space between a square tube and a rigid tube located in its center, and concluded that average Nusselt number is affected by the volume fraction of nanoparticles in the base fluid. The major subject in some other studies, as well as the current one, is study of thermal and hydrodynamic behavior of water-AL_2O_3 nanofluid flow in a channel with non-circular cross-section, containing a middle rigid body and holder plate. In addition, the effects of Reynolds number, Prandtl number, concentration of nanoparticles, and inlet temperature are addressed.

In the present work, water-AL_2O_3 nanofluid flow is considered in a rectangular cross-section channel (H×H, H=0.05 m) with an inner circular tube (D=0.025m). Table 1 indicates the thermophysical properties of AL_2O_3 nanoparticles. Figure 1 shows the schematic of the problem. The flow is assumed to be laminar, incompressible and steady with constant properties. The channel walls are exposed to a constant thermal flux of 20,000 w/m². Inlet fluid temperature is 293 K. Moreover, holder plates and middle rigid tubes are considered to be isolated. The Reynolds number is Re=100, 250, and 500. In addition, the flow is uniform in the inlet and is hydro-dynamically fully-developed along the tube direction. Figure 2 presents the geometries are used in the current study. This numerical study aims to compare the effects of holder plates on fluid convective heat transfer and flow pattern

Table 1. Thermophysical properties of AL_2O_3 nanoparticles

Average particle diameter[nm]	density[kg/m³]	C_p [Kj/kg.K]	K [W/m.K]
20	3970	765	25
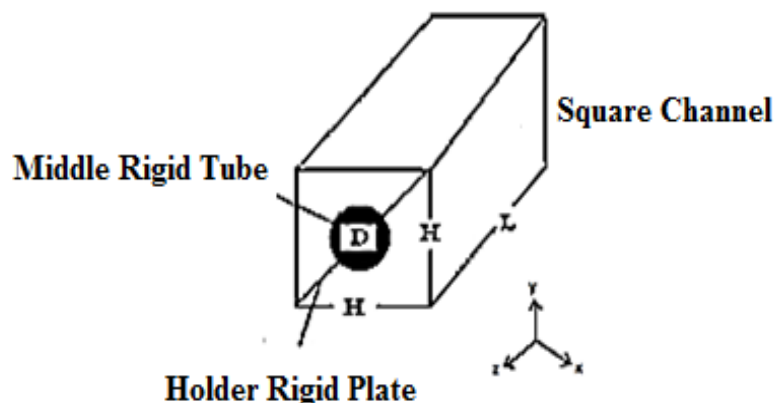
Figure 1. Schematic of the problem

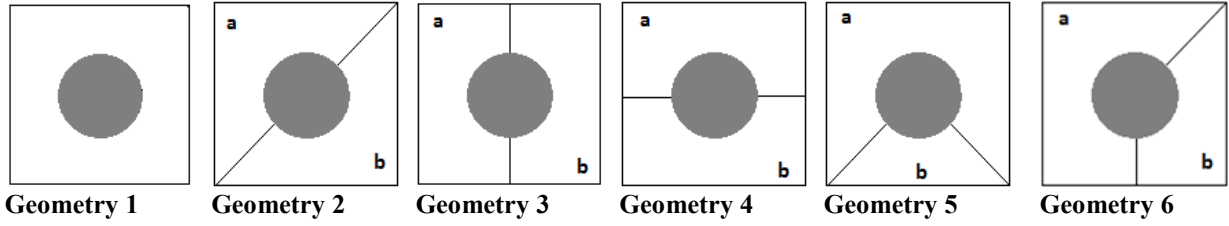Geometry 1   Geometry 2   Geometry 3   Geometry 4   Geometry 5   Geometry 6

Figure 2. Different positions of holder plates.

MATHEMATICAL MODEL AND VALIDATION

By neglecting thermal loss, viscous loss, radiation, and gravity and assuming Newtonian and incompressible fluid in this study, the governing equations for three dimensional laminar flow inside a channel are as follows [14-16]:

Continuity equation:

$$\frac{\partial u}{\partial x} + \frac{\partial v}{\partial y} + \frac{\partial w}{\partial z} = 0 \tag{1}$$

Momentum equation in the X- direction:

$$u\frac{\partial u}{\partial x} + v\frac{\partial u}{\partial y} + w\frac{\partial u}{\partial z} = -\frac{1}{\rho}\frac{\partial p}{\partial x} + \frac{\mu}{\rho}\left(\frac{\partial^2 u}{\partial x^2} + \frac{\partial^2 u}{\partial y^2} + \frac{\partial^2 u}{\partial z^2}\right) \tag{2}$$

Momentum equation in the Y- direction:

$$u\frac{\partial v}{\partial x} + v\frac{\partial v}{\partial y} + w\frac{\partial v}{\partial z} = -\frac{1}{\rho}\frac{\partial p}{\partial y} + \frac{\mu}{\rho}\left(\frac{\partial^2 v}{\partial x^2} + \frac{\partial^2 v}{\partial y^2} + \frac{\partial^2 v}{\partial z^2}\right) \tag{3}$$

Momentum in the Z- direction:

$$u\frac{\partial w}{\partial x} + v\frac{\partial w}{\partial y} + w\frac{\partial w}{\partial z} = -\frac{1}{\rho}\frac{\partial p}{\partial y} + \frac{\mu}{\rho}\left(\frac{\partial^2 w}{\partial x^2} + \frac{\partial^2 w}{\partial y^2} + \frac{\partial^2 w}{\partial z^2}\right) \tag{4}$$

Energy equation:

$$u\frac{\partial T}{\partial x} + v\frac{\partial T}{\partial y} + w\frac{\partial T}{\partial z} = \alpha\left(\frac{\partial^2 T}{\partial x^2} + \frac{\partial^2 T}{\partial y^2} + \frac{\partial^2 T}{\partial z^2}\right) \tag{5}$$

Fluid thermal diffusivity is defined as follows [17]:

$$\alpha = \frac{K}{\rho C_p} \tag{6}$$

Reynolds and Prandtl numbers are defined as follows [18]:

$$Re = \frac{\rho V D_H}{\mu} \tag{7}$$

$$pr = \frac{\mu}{\rho \alpha} \tag{8}$$

Hydraulic diameter is the characteristic length employed in open channels or channels with non-circular cross-sections. The hydraulic diameter is calculated by the following equation:

$$D_H = \frac{4A}{P} \tag{9}$$

$$A = \frac{1}{2}[(H \times H) - (\pi r^2)] \tag{10}$$

$$P = [(2 \times H) + (\pi \times r) + \sqrt{H^2 + H^2} - 2 \times r] \tag{11}$$

Where A is wetted cross-section, P is wetted perimeter of the cross-section, H is edge size of the cross-section, and r is the radius of the inner tube. Equation 12 is used to specify the mean temperature of the fluid.

$$T_{bulk} = \frac{(q'' z\, p)}{(\dot{m} c_p)} + T_{in} \tag{12}$$

Also, mass flow rate, convective heat transfer coefficient, Nusselt number, friction factor and inlet velocity are defined as follows:

$$\dot{m} = \rho A V \tag{13}$$

$$h = \frac{q''}{T_{wall} - T_{bulk}} \tag{14}$$

$$Nu = \frac{h D_H}{k} \tag{15}$$

$$f = \frac{\tau_{wall}}{\frac{1}{2}\rho v^2} \tag{16}$$

$$V = \frac{Re \mu}{\rho D_H} \tag{17}$$

Structure grid is employed to examine the grid resolution test. The grid is uniform along the channel and proportionally finer in the inlet, outlet, corners (near walls), and curved surface. To investigate the dependency of numerical solution results from grid point's number, four types of meshes, namely coarse, medium, fine and very fine are studied (Fig. 3). The figure shows that two grids with 135000 and 156000 cells lead to similar results. To decrease the calculation costs, a rectangular mesh with 1,350,000 cells and 1,395,436 nodes is selected.
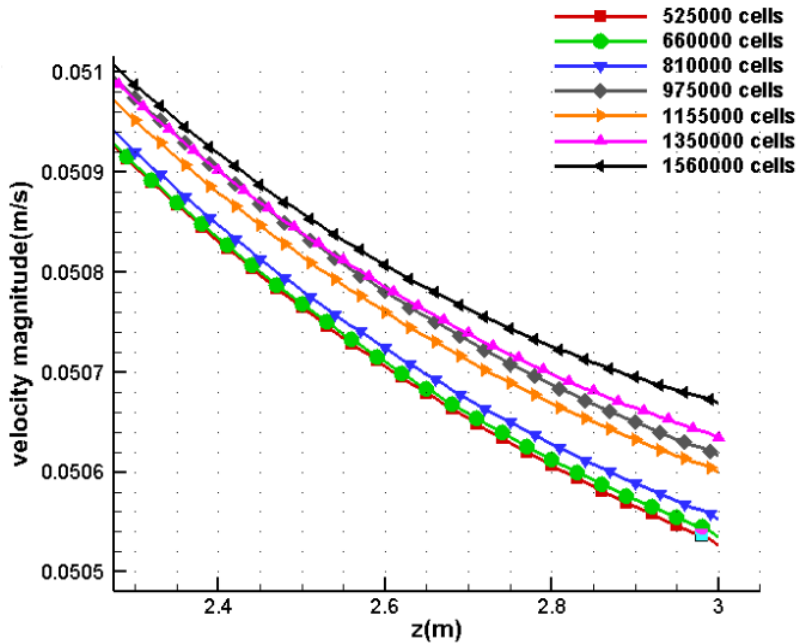

Figure 3. Velocity along the channel for different number of grid cells

The results are compared to the reference [11] and [14] for validation. Obtained average Nusselt number and Re×f are compared with their results (Table 2). It is found that our simulations have sufficient accuracy to predict thermal and hydrodynamic behavior of the fluid flow.

**Table 2.** Average Nusselt number and Re×f for pure water flow through a channel

Percentage error	Present work	Mehrzad &Kalteh [14]	Shah & London [11]
3.328	Nu=5.14	Nu=5.6615	Nu=5.317
1.316	f.Re=22.31	f.Re=24.054	f.Re=22.02

RESULTS AND DISCUSSION

According to figures 4, 5, and 6, the maximum velocity is observed in the middle of channel cross section, away from holder plates. This is due to low shear stress in this region. In addition, different geometries are introduced for discussion.

Since gravity effect is neglected in the current study, similar results are obtained for geometries 3 and 4. The holder plate in the channel divides the volume of flowing fluid into two parts; however, the Reynolds number and flow regime are similar for all cases.

It can be seen that when the holder plate is in line with the symmetry line, higher velocity is obtained for smaller volume size of the duct, such as geometries 5 (a, b) and 6 (a, b). In all Reynolds number in this study, the highest and lowest velocities were obtained in the middle of Geometries 5 (b) and 1, respectively. Regarding the provided contours, they have different values at different Reynolds number.
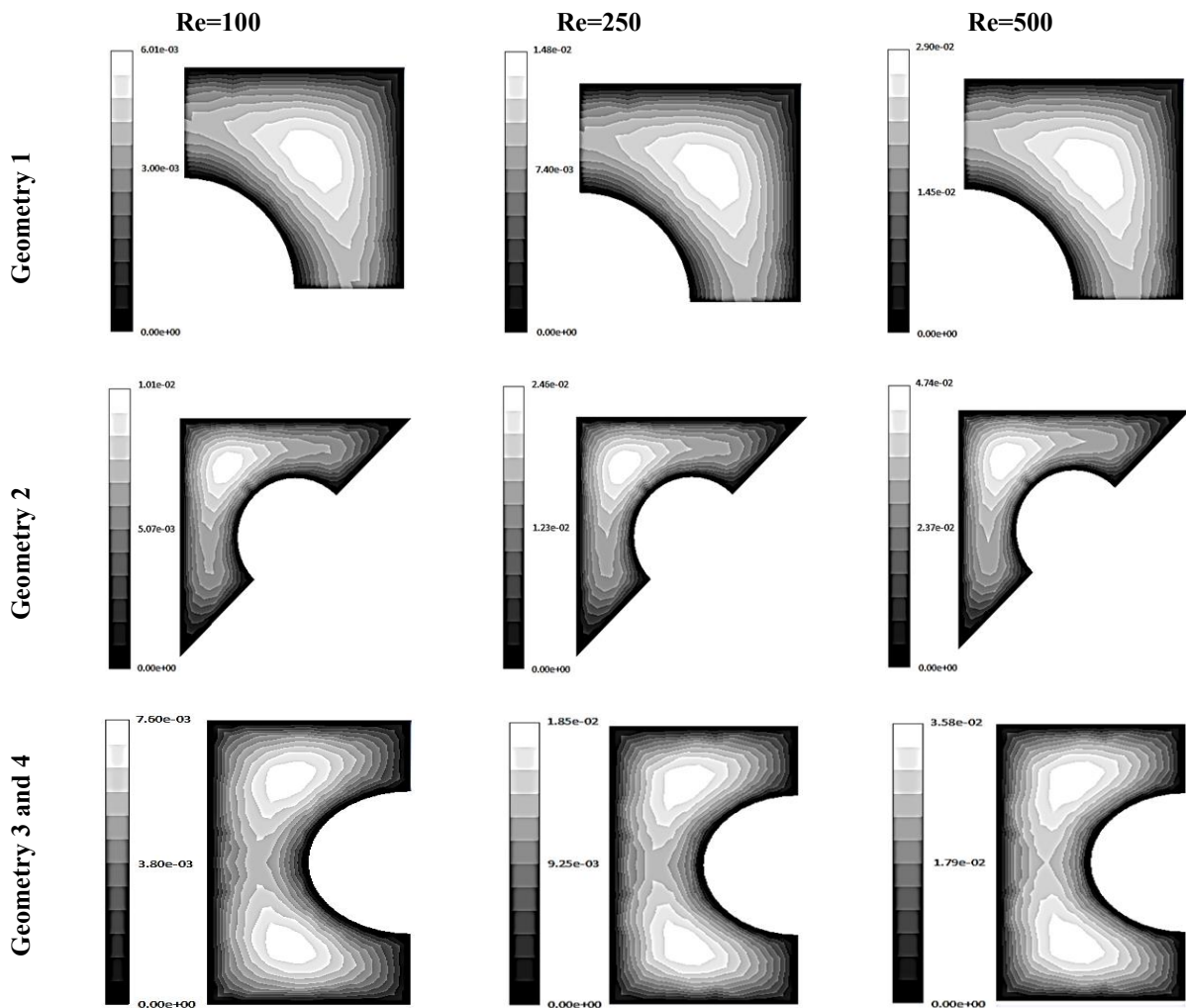
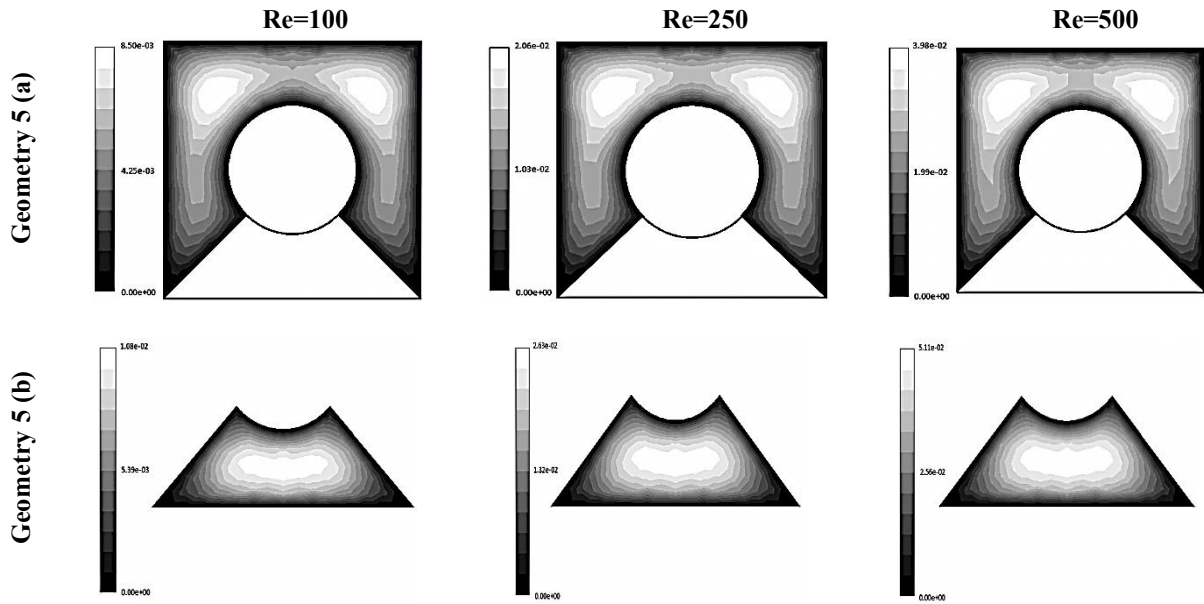**Figure 4.** Streamlines for geometries 1, 2, 3, and 4

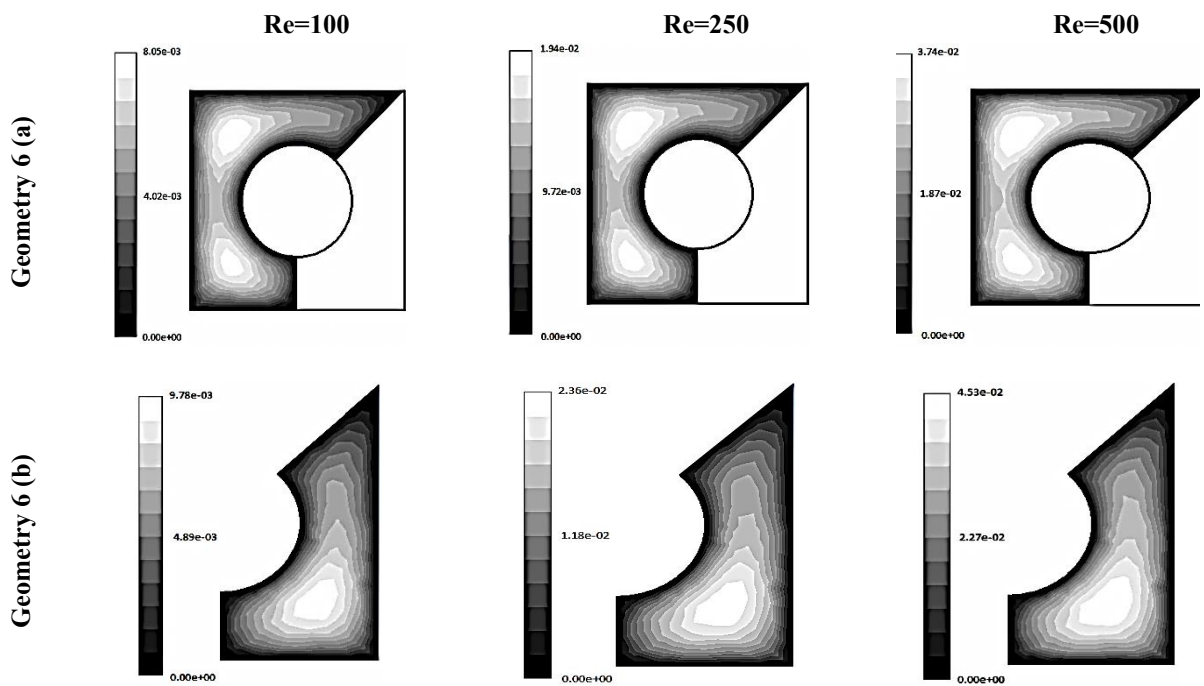**Figure 5**. Streamlines for geometry 5

Figure 6. Streamlines for geometry 6

The interesting point is that different outlet velocities can be obtained in this case at the same time under the same flow regime at constant Reynolds numbers. Its rate depends on the position of the holder plate. For example, the highest velocity for sections *a* and *b* of geometry 6 at Re=100 are 0.00805 (m/s) and 0.00978 (m/s), respectively. In addition, the highest velocity for sections *a* and *b* of geometry 6 at Re=500 are 0.0374 (m/s) and 0.0453 (m/s), respectively. As shown, when the holder plate is in line with the symmetry line of the channel, fluid flow has similar hydrodynamic behavior at both sides of the plate.

Figures 7, 8, and 9 present the isothermal line for the outlet section of the flow for different geometries. According to these figures, holder plate allows for different temperature in the outlet cross-section of the channel

at the same time under the same flow regime and in the same duct. Moreover, the highest temperature occurs around the holder plate.
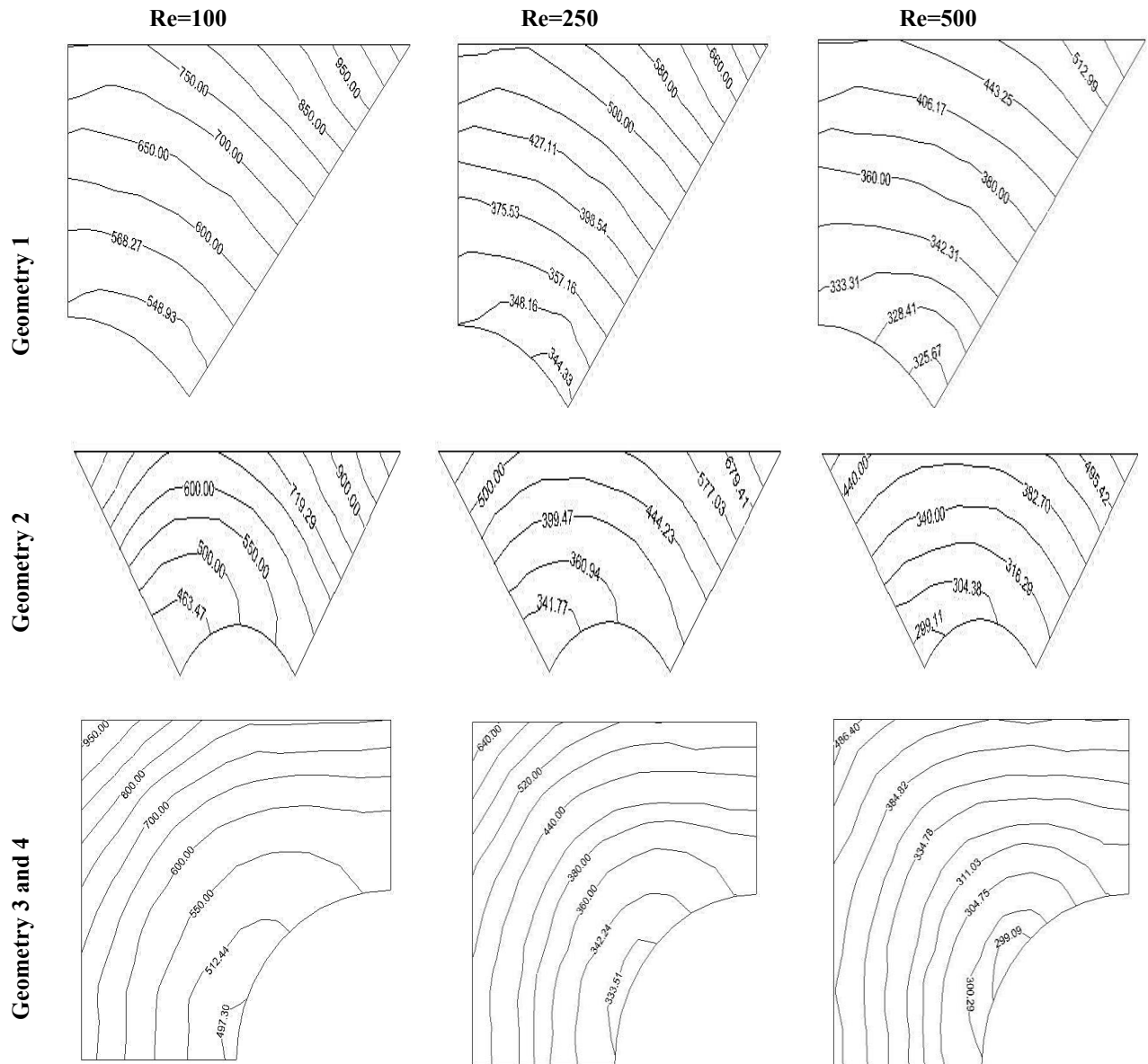
Figure 7. Temperature lines in outlet cross-section of flow for geometries 1, 2, 3, and 4

Figure 10 presents the average convective heat transfer for different Reynolds numbers. At Re=100, the highest and lowest h are observed for Geometries 5 (b) and 1, which were equal to 73.11 and 33.87, respectively. For Geometries 2 (a, b), 3, 4, and 5 (a), the mean values of h are very close to each other and equal to 59.11, 58, 93, and 58.56, respectively.

At Re=250, the highest and lowest mean values of h are observed for Geometries 5 (b) and 2 (a, b), which are equal to 181.2 and 130.01, respectively. The highest and lowest mean values of h occur at Re=500 for the same geometries at Re=100 (Figure 10).

Researchers tend to evaluate the pressure drop required for maintaining internal flows. Figure 11 presents the pressure drop as a function of channel length. The highest and lowest values of the pressure drop occur for the Geometries 5 (b) and 1, respectively.
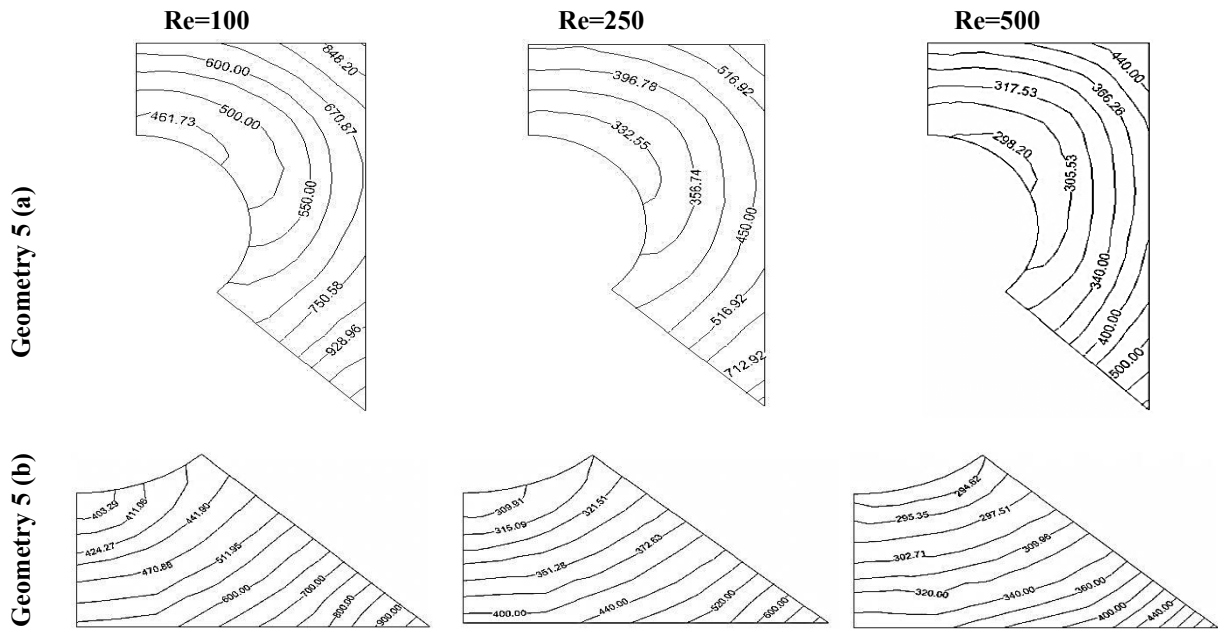
Re=100   **Re=250**   **Re=500**

Figure 8. Temperature lines in outlet cross-section of flow for geometry 5

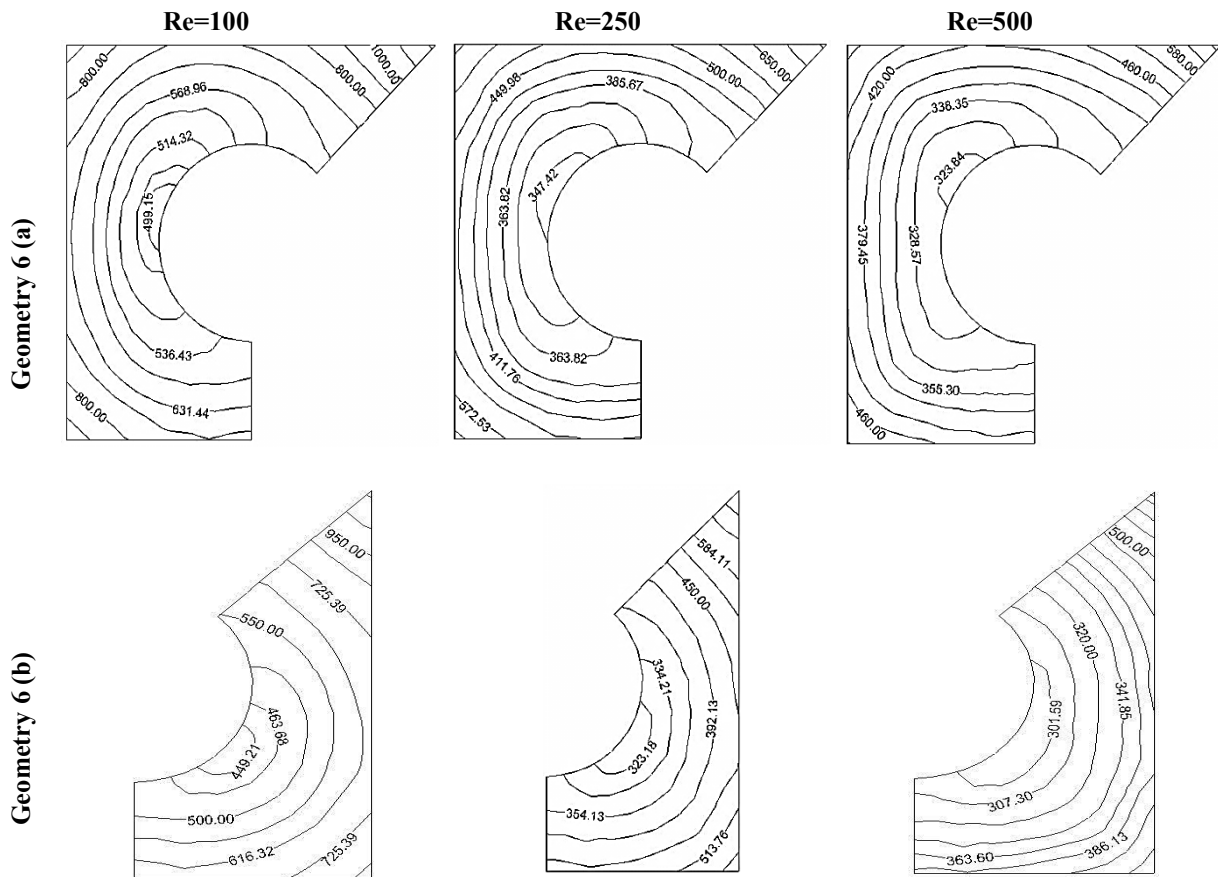**Re=100**   **Re=250**   **Re=500**

Figure 9. Temperature lines in outlet cross-section of flow for geometry 6
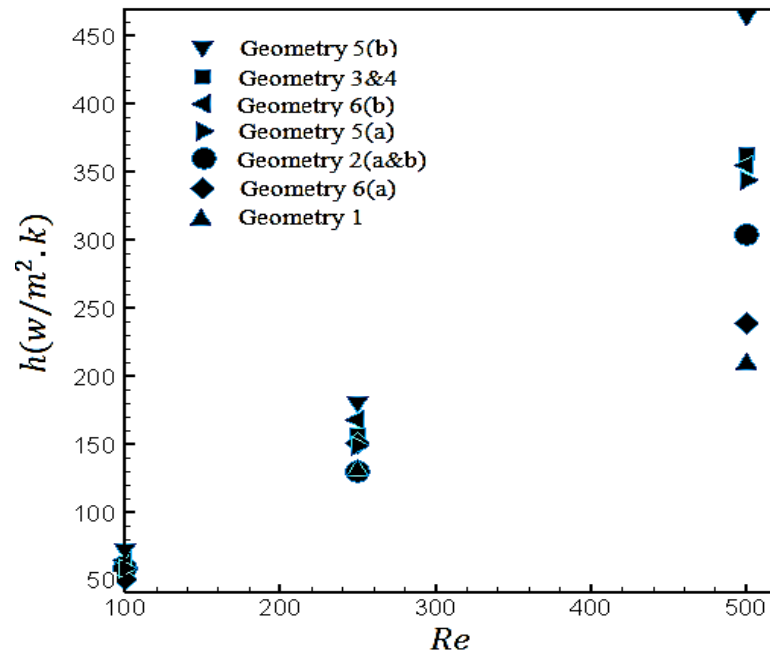
Figure 10. Comparison of mean convective heat transfer for different Reynolds numbers
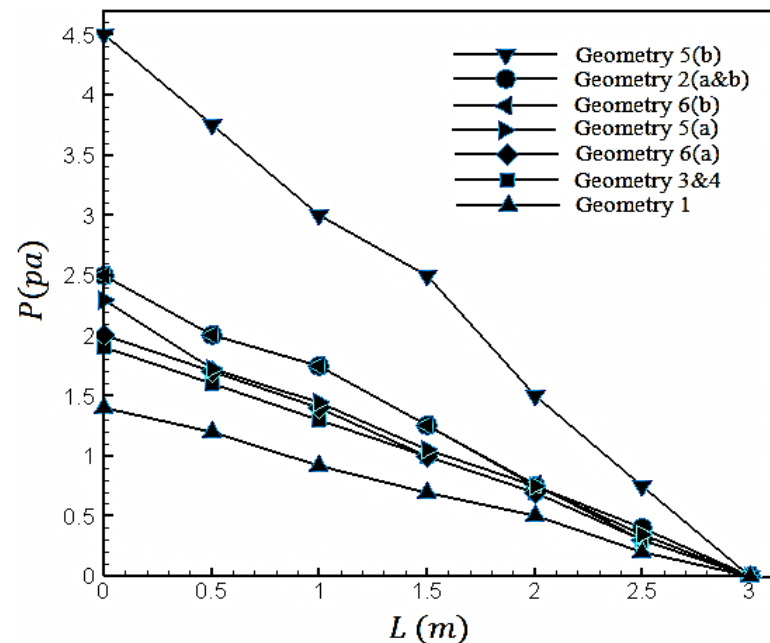

Figure 11. Comparison of the pressure drop versus the channel length

Figure 12 presents fluid mass temperature (bulk temperature, T_{bulk}) at different Reynolds numbers. The mean temperature is used to explain thermal behavior of internal flows in the absence of constant free flow temperature. Bulk temperature is defined in a certain transversal cross-section based on thermal energy transferred by the fluid passing through that section. It is observed that the wall temperature around the perimeter of a non-circular section cross-section changes under a uniform thermal flux conditioning. It is expected that the ratio of fluid temperature to its inlet temperature increases by moving the fluid along the channel. In this problem, the highest T_{bulk} at Re = 100, 250, and 500 corresponds to the Geometry 1, which are equal to 517, 387.42, and 345.313 K, respectively. The lowest temperature at Re=100, 250, and 500 was obtained for the Geometry 5 (b) that are equal to 444.53, 387.42, and 500, respectively.
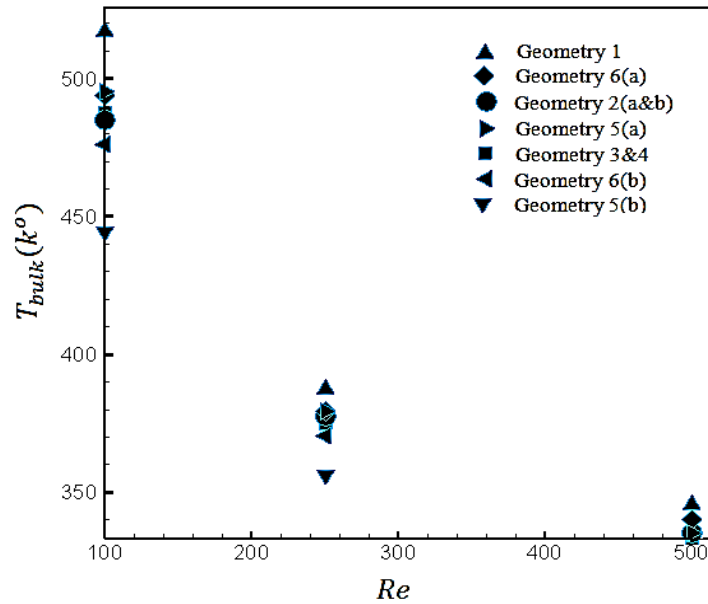
Figure 12. Comparison of fluid mass temperature at different Reynolds numbers

CONCLUDING REMARKS

In the present work, the convective heat transfer of water-AL$_2$O$_3$ nanofluid in the space between a square channel and middle rigid plate for different positions of the holder plate was investigated. The results indicated that the position of holder plate has significant effects on the flow behavior. When this plate is not located in the line of symmetry of the channel cross-section, it can produce two flows with different velocities and outlet temperatures at the same time under the same inlet conditions. When the holder plate is in line with the symmetry line of the channel, fluid flow has similar hydrodynamic behavior at both sides of the plate. Finally, the studies of Erdinc and Yilmaz [21] is proposed to compare the present results with the results for the case of converging and diverging channels.

NOMECLATURE

A	Area [m^2]
C$_p$	Specific thermal coefficient [kJ/kg.K]
D$_H$	Hydraulic diameter [m]
h	Convective heat transfer coefficient [W/m^2.K]
k	Thermal conductivity [W/m.K]
ṁ	Mass flow rate [kg/s]
Nu	Nusselt number
p	Pressure [Pa]
Pr	Prandtl number
Re	Reynolds number
T	Temperature [K]
u	x-component of the velocity field [m/s]
v	y-component of the velocity field [m/s]
w	z-component of the velocity field [m/s]
α	Thermal expansion coefficient [1/K]
ρ	Density [W/m^2]
μ	Viscosity [Pa. s]

REFERENCES

[1] Choi. S.U.S., Eastman. J.A. (1995). Enhancing thermal conductivity of fluids S with nanoparticles. In Developments and Applications of Non-Newtonian Flows. Volume FED-231/MD-66. Siginer DA, Wang HP, editor. ASME, New York, 99–105.
[2] Murshed SS, De Castro CN. (2011). Forced convective heat transfer of nanofluids in minichannels. InTwo Phase Flow, Phase Change and Numerical Modeling. InTech.

[3] Mirmasoumi. S , Behzadmehr. A. (2008). Numerical study of laminar mixed convection of a nanofluid in a horizontal tube using two-phase mixture model. Applied Thermal Engineering.;28(7). 717-27.

[4] Pishkar. I, Ghasemi. B. (2012). Effect of nanoparticles on mixed convection heat transfer in a horizontal channel with heat source. Modares Mechanical Engineering. 12(2):95-108.

[5] Vasefi. I, Alizadeh. M. (2013). A numerical investigation of CuO–water nanofluid in different geometries by two-phase Euler–Lagrange method. World Appl Sci J. 26(10). 1323-9.

[6] Heris. SZ, Talaii. E, Noie. SH. (2012). CuO/water nanofluid heat transfer through triangular ducts. Iran. J. Chem. Eng.;9(1). 23-32.

[7] Ho. CJ, Chen. MW, Li. ZW. (2008). Numerical simulation of natural convection of nanofluid in a square enclosure: effects due to uncertainties of viscosity and thermal conductivity. International Journal of Heat and Mass Transfer. 51(17). 4506-16.

[8] Ben Mansour. R, Galanis. N, Nguyen.(2009). CT. Developing laminar mixed convection of nanofluids in an inclined tube with uniform wall heat flux. International Journal of Numerical Methods for Heat & Fluid Flow. 19(2). 146-64.

[9] Nguyen. CT, Roy. G, Gauthier. C, Galanis. N.(2007). Heat transfer enhancement using Al 2 O 3–water nanofluid for an electronic liquid cooling system. Applied Thermal Engineering. 27(8):1501-6.

[10] Heris. SZ, Esfahany. MN, Etemad. G. (2007). Numerical investigation of nanofluid laminar convective heat transfer through a circular tube. Numerical Heat Transfer, Part A: Applications. 52(11). 1043-58.

[11] Shah. RK, London. AL. (2014). Laminar flow forced convection in ducts: a source book for compact heat exchanger analytical data. Academic press.

[12] Zhang. LZ. (2007). Laminar flow and heat transfer in plate-fin triangular ducts in thermally developing entry region. International Journal of Heat and Mass Transfer. 50(7). 1637-40.

[13] Heyhat. MM, Kowsary. F. (2010). Effect of particle migration on flow and convective heat transfer of nanofluids flowing through a circular pipe. Journal of Heat Transfer. 132(6). 062401.

[14] A. Bejan. (2013). Convection Heat Transfer, 4th Edition, Wiley.

[15] Pak. BC, Cho. YI. (1998). Hydrodynamic and heat transfer study of dispersed fluids with submicron metallic oxide particles. Experimental Heat Transfer an International Journal. 11(2). 151-70.

[16] Hamilton. RL, Crosser. OK.(1962). Thermal conductivity of heterogeneous two-component systems. Industrial & Engineering chemistry fundamentals. 1(3). 187-91.

[17] Kalteh. M, Abbassi. A, Saffar-Avval. M, Frijns. A, Darhuber. A, Harting. J. (2012). Experimental and numerical investigation of nanofluid forced convection inside a wide microchannel heat sink. Applied Thermal Engineering. 36. 260-8.

[18] Chon. CH, Kihm. KD, Lee. SP, Choi. SU. (2005). Empirical correlation finding the role of temperature and particle size for nanofluid (Al 2 O 3) thermal conductivity enhancement. Applied Physics Letters. 87(15). 153107.

[19] Nguyen. CT, Desgranges. F, Roy. G, Galanis. N, Maré. T, Boucher. S, Mintsa. HA. (2007). Temperature and particle-size dependent viscosity data for water-based nanofluids–hysteresis phenomenon. International Journal of Heat and Fluid Flow. 28(6):1492-506.

[20] Sieder. EN, Tate. GE. (1936). Heat transfer and pressure drop of liquids in tubes. Industrial & Engineering Chemistry. 28(12). 1429-35.

[21] Erdinc. MT, Yilmaz. T. (2018). Numerical Investigation of Flow and Heat Transfer in Communicating Converging and Diverging Channels, Journal of Thermal Engineering, 4(5), 2318-2332.